Title

RESONANCE RAMAN SPECTROSCOPY OF Mn(III) ETIOPORPHYRIN I AT THE n --> n* and CHARGE TRANSFER BANDS: THE USE OF CHARGE TRANSFER BANDS TO MONITOR THE COMPLEXATION STATE OF METALLOPORPHYRINS

Permalink

https://escholarship.org/uc/item/5s42v25g

Author

Asher, Sanford

Publication Date

1975-09-01

Submitted to Journal of Chemical Physics

LBL-4254
Preprint c.1

RESONANCE RAMAN SPECTROSCOPY OF Mn(III) ETIOPORPHYRIN I AT THE $\pi \rightarrow \pi^*$ AND CHARGE TRANSFER BANDS: THE USE OF CHARGE TRANSFER BANDS TO MONITOR THE COMPLEXATION STATE OF METALLOPORPHYRINS

Sanford Asher and Kenneth Sauer

September 1975

Prepared for the U. S. Energy Research and Development Administration under Contract W-7405-ENG-48

LBL-4254 c.1

DISCLAIMER

RESONANCE RAMAN SPECTROSCOPY OF Mn(III) ETIOPORPHYRIN I AT THE $\pi \rightarrow \pi^*$ AND CHARGE TRANSFER BANDS: THE USE OF CHARGE TRANSFER BANDS TO MONITOR THE COMPLEXATION STATE OF METALLOPORPHYRINS

Sanford Asher and Kenneth Sauer

Department of Chemistry and

Laboratory of Chemical Biodynamics

University of California

Berkeley, California 94720

Abstract

Electronic transitions of Mn(III) etioporphyrin I (MnETP) are assigned by the use of resonance Raman spectroscopy (RRS). Dramatic differences are found in the RR spectra of MnETP upon excitation within different absorption bands. RRS supports the assignment of the strong absorption band of Mn(III) porphyrins between 460-490 nm to a charge transfer transition. The two bands between 540-600 nm are assigned to vibronic components of a $\pi \rightarrow \pi^*$ transition. The RR spectra of MnETP-X ($X=F^-, Cl^-, Br^-, I^-$ or butanol) show large differences in the low energy Raman spectrum (100-500 cm^{-1}) depending on the axial ligand. Pure Mn-halide vibrations are assigned. An explanation is proposed to account for the differences between the RR spectra excited in the Q bands and the charge transfer band. Some of the vibrational Raman bands in the low energy region may serve as probes for the degree of out-of-plane distortion of the metal from the porphyrin plane.

I. INTRODUCTION

Resonance Raman spectroscopy has been utilized as a probe of the porphyrin environment in hemoglobin[1-5], cytochrome c[1,6-9] and in Co substituted hemoglobin[10]. In addition, the resonance Raman spectra of various metalloporphyrins[11-17] and free base porphyrins[18,19] have been investigated. From this research, it appears that excitation within $\pi \rightarrow \pi^*$ electronic transitions involving the macrocyclic ring enhances vibrations within the macrocycle[1-3,6,13,18,19]. The vibrations of atoms that are not intimately conjugated to the aromatic structure of the ring make only a small contribution to the resonance Raman spectrum; and as a result, changes in peripheral substituents about the porphyrin ring produce relatively small differences in the vibrational frequencies observed[12,13,19]. The alterations of the resonance Raman spectra produced by changes in peripheral substituents appear to be induced mainly by changes in the symmetry of the porphyrin macrocycle[13].

Changes in the central metal also result in differences in the RR spectra. Variations in the spin state, oxidation state[1,2,5,6] or in the planarity of the metal with respect to the porphyrin plane shift the energy and polarization of some of the resonance enhanced vibrations[10,11,15,16]. These shifts in energy and polarization are due to a change in the structure, which may be a doming of the porphyrin when the metal lies farther from the porphyrin ring plane[1,2,5,6,15] or an expansion of the porphyrin core resulting in a decrease of the metal-to-porphyrin-center distance[16]. The effect of axial ligation on porphyrin macrocycle vibrations depends on the extent that the ligand induces a change in the displacement of the metal from the ring plane[15].

Prior to this report, the only feature directly sensitive to the environment of the porphyrin macrocycle was the dispersion with respect to frequency of the depolarization ratio. Since the depolarization ratio is a function of porphyrin symmetry, it can be influenced by environmental factors such as axial ligation[11,15] and peripheral substitution[8,13,14].

This report is a systematic study of metal-dependent vibrations which are enhanced by excitation within the charge transfer band of Mn(III) etioporphyrin I (MnETP). We find that the resonance Raman bands enhanced by excitation within the charge transfer absorption band correspond to vibrations associated with the central metal. This is in contrast to the porphyrin macrocycle vibrations which are resonance enhanced by excitation within the Q bands. This feature permits observation of metal-axial ligand vibrations. The vibrations involving the central metal occur at relatively low energies, $<500\ cm^{-1}$. By studying the effects of changing the axial ligand, vibrations may be assigned to particular parts of the porphyrin. Vibrations with significant metal contribution will be affected by a change in the axial ligand more than will vibrations that are associated mainly with the porphyrin ring. The intensity of some of these vibrations appears to be sensitive to the coplanarity of the metal and the porphyrin ring; this permits the resolution of metal-ligand vibrations as well as the detection of subtle changes in the geometry of the porphyrin.

II. EXPERIMENTAL

A. Materials

Samples of manganese etioporphyrin I acetate were kindly supplied by Dr. Melvin Calvin. The visible, UV and near IR absorption spectra correspond to those in the literature[20]. Thin layer chromatography performed on the MnETP using a 1:1 pyridine-water solution on a cellulose plate demonstrated the presence of only one component.

The halogen salts of MnETP were prepared from a methanol solution of MnETP containing the sodium salt of the halide. Water was added dropwise with stirring. The resulting precipitate was washed repeatedly with water and centrifuged. The halide salts were dried under vacuum, and their absorption spectra were subsequently monitored (Table I). The spectra of all of the halides of MnETP except for the fluoride agreed with those in the literature[20]. The absorption peaks of the fluoride complex in chloroform were 2-6 nm to higher energy from the values reported by Boucher[20]. The intensity ratio of band V/VI (R in Boucher's nomenclature[20]) was also 80% higher. It should be noted that there is a large variation in the value of R as the axial ligand is changed from I^- to Br^- to Cl^-.[20] The change that Boucher observes in going to F^- is surprisingly low. In addition, the chloroform solutions of MnETP-F were labile. With time our samples exhibited absorption changes toward the values reported by Boucher. The MnETP-F salt that we have prepared gives the characteristic spectrum of MnETP complexes in coordinating solvents such as methanol and pyridine. The $Na^{35}Cl$ (99.35%) and $Na^{37}Cl$ (90.36%) were obtained from Oak Ridge National Laboratories.

B. Methods

The Raman spectra recorded with excitation at 568.2 and 530.9 nm and the Raman spectrum of MnETP acetate in butanol with excitation at 457.9 nm were measured through the courtesy of Dr. James Scherer at Western Regional Laboratories, USDA, Albany, California[21]. Excitation at 568.2 and 530.9 nm were obtained from a Spectra Physics Model 165-01 Kr^+ laser. Excitation at 457.9 nm was obtained from a Coherent Radiation Model 52 Ar^+ laser. The remaining spectra were measured using an instrument belonging to Dr. H. Strauss at the University of California-Berkeley, Department of Chemistry. A Coherent Radiation model CR2 Ar^+ laser was coupled to a Spex 1401 double monochromator.

The incident laser beam was chopped, and the scattered light was amplified with synchronous detection.

The samples were dissolved in CS_2, $CHCl_3$ (previously distilled from anhydrous P_2O_5) or n-butanol, introduced into melting point capillaries and sealed. Excitation was transverse to the viewing direction and the polarization of the scattered light was scrambled before introduction into the monochromator. Depolarization ratios were measured by passing the scattered light through a Polaroid analyzer prior to the scrambler. Absorption spectra were measured on a Cary 14 recording spectrophotometer.

III. RESULTS

The visible and near UV absorption spectrum of Mn(III) ETP acetate in n-butanol is shown in Fig. 1. The bands are labeled using the numbering scheme introduced by Boucher[20,22] and the locations are shown for the laser lines used to excite the resonance Raman spectra shown in Fig. 2. The laser line at 568.2 nm lies between bands III and IV, while the line at 530.9 nm lies on the high energy side of band IV. The 457.9 nm line is in resonance with peak V, an electronic transition that has been assigned as a possible charge transfer transition[20,22]. The solvent contributions to the Raman spectra are noted in the figures. Table II contains the energies and relative intensities for each of the Raman peaks shown in Fig. 2.

Apart from the rising baseline, the spectra shown in Figs. 2a and b are qualitatively similar. At present it is unclear whether the rising baseline in Fig. 2a which peaks at 15,900 cm^{-1} (630 nm) represents emission from MnETP or an impurity, but there are no obvious features in the absorption spectrum that would give rise to fluorescence at this wavelength.

The Raman spectra shown in Figs. 2a and b show strong correlations in frequency and intensity. However, differences appear for peaks at 757, 988 and 1313 cm^{-1}. The intensities of these three peaks show greater enhancement with excitation in band III than with excitation in band IV. Conversely, the peak at 1374 cm^{-1} is more intense with excitation in band IV rather than in band III. The most intense features of both spectra appear between 1550 and 1650 cm^{-1}. There are few well resolved features below 500 cm^{-1}.

Comparision of the spectra obtained with excitation in bands III and IV with the spectrum obtained with excitation in band V show more dramatic differences. The most intense features in Fig. 2c are vibrations at frequencies less than 500 cm^{-1}. This is the region in which manganese-pyrrole nitrogen vibrations are expected to occur[23,24,25]. Higher energy vibrations are still visible, but their relative intensities are small. A number of peaks are conspicuous by their absence. The bands at 757 and 1002 cm^{-1} seen in Figs. 2a and 2b do not appear with excitation in absorption band V; instead a new peak appears at 1502 cm^{-1}.

In order to determine whether the low energy vibrations (less than 500 cm^{-1}) in the Raman spectrum of MnETP are metal related, the Raman spectra of the F^-, Cl^-, Br^-, and I^- salts were measured. These Raman spectra are shown in Fig. 3. Table III lists the frequencies and relative intensities of the Raman bands of MnETP-X between 100 and 500 cm^{-1}. All of the Raman bands in Fig. 3 are polarized. Carbon disulfide was used as the solvent for the F^-, Cl^-, and Br^- salts. Because of insufficient solubility in CS_2, chloroform was used for the I^- salt. The exciting laser light was changed in order to stay in maximum resonance with peak V.

The Raman spectra of the halide salts are clearly a function of the axial ligand. Unique peaks appear for each of the halide salts. A number of important differences and similarities appear among these spectra.

The similarities will be discussed first. In the Raman spectra of all of these complexes peaks appear at about 398, 374, 342, 327 and 260 cm^{-1}, and these frequencies are virtually independent of the mass of the axial ligand. The 260 cm^{-1} peak decreases by 1 cm^{-1} from the F^- to the Cl^- complex and appears as a shoulder near 260 cm^{-1} for the Br^- complex. The Raman spectrum of the solvent, $CHCl_3$ masks this region in the I^- complex. The spectrum of MnETP in butanol (Fig. 2c) shows a peak appearing at 266 cm^{-1}.

The relative intensity of the 329 cm^{-1} peak is found to be sensitive to the axial ligand. A distinct increase in intensity occurs as the axial ligand is changed from F^- through I^-. The 329 cm^{-1} peak is not evident for MnETP in butanol. Because the peaks at 329 and 342 cm^{-1} both show a small frequency dependence on the ligand, there must be some metal contribution to these vibrational modes. The change in axial ligand has a small effect through the metal but, because the effects are small, these modes must also have a large porphyrin contribution. The peak at about 400 cm^{-1} appears in all of the spectra. The exact position is difficult to obtain since a very weak Raman line of CS_2 also appears in this region. The position of this peak does not appear to shift appreciably with a change in the ligand, since this peak appears at 398 cm^{-1} for MnETP in butanol and at 398 cm^{-1} for the I^- complex in $CHCl_3$.

A number of peaks do not correlate between spectra. The peak at 495 cm^{-1} in the F^- complex does not have any counterpart in the other spectra. The 285 cm^{-1}, 225 cm^{-1} and 165 cm^{-1} peaks in the Cl^- complex also show no counterparts in the other spectra. This is also true of the 245 and 143 cm^{-1} peaks of the Br^- and the 186 and 118 cm^{-1} peaks of the I^- complex. The peaks at 495 in the F^-, 285 in the Cl^-, 245 in the Br^- and 233 in the I^- appear to correspond with Mn-X vibrations observed in the far IR spectra of Mn(III) protoporphyrin IX dimethyl ester halides[26]. All of these peaks are shifted between 43 and 23 cm^{-1} to higher energy from the Mn-halide stretches in Mn(III) protoporphyrin IX dimethyl ester which appear at 462, 262, 211 and 190 cm^{-1} for F^-, Cl^-, Br^- and I^- respectively, presumably because the spectra in this report are for the molecules in solution rather than in the solid state mulls that were used for the far IR spectral measurements.

Another indication that these peaks represent the Mn-halide stretches is shown by isotopic substitution of ^{35}Cl and ^{37}Cl in the MnETP-Cl complex (Fig. 4 and Table IV). All of the low energy peaks are constant in energy, within experimental precision $\pm$ 1 cm^{-1}, except for the peaks at 285 and 225 cm^{-1} (Table IV). The peaks at 285 and 225 cm^{-1} show a shift of 4 and 2.6 cm^{-1}, respectively, to lower energy when the axial ligand is changed from ^{35}Cl to ^{37}Cl. Using a harmonic oscillator model, the energy shift for the 285 cm^{-1} peak is 0.8 cm^{-1} less than the shift of 4.8 cm^{-1} expected if this were a pure Mn-Cl vibration. The peak at 225 cm^{-1} shows a smaller shift, and the vibrational mode responsible for it must also involve motion of the metal against the porphyrin macrocycle.

The peaks at 165 and 143 cm^{-1} in the Cl^{-1} and Br^{-1} complexes and the two peaks at 186 and 118 cm^{-1} in the I^- complex appear also to be axial-ligand dependent. The 165 cm^{-1} peak, the dominant feature in the Raman spectrum of the Cl^- complex, shows no energy change with isotopic substitution. A correlation of the 225 cm^{-1} peak in Cl^- with the 143 cm^{-1} peak in Br^- and the 118 cm^{-1} peak in I^- seems reasonable. The peaks exhibit a decrease in energy with mass and may reflect a vibration of the metal and halide against the porphyrin. Although the corresponding peak is not apparent in the F^- complex, it may lie within the broad feature at 260 cm^{-1}. This is supported by a polarization study in which the RR peaks recorded with the analyzer oriented either parallel or perpendicular to the electric vector of the incident radiation showed different maxima separated by about 3 cm^{-1}.

Table V summarizes the assignments for the low energy region of the Raman spectra of the halide complexes of MnETP. The peaks at 193, 179 and 186 cm^{-1} in the F^-, Cl^- and I^- complexes are currently under study and will be described in a subsequent report.

The higher energy region 500-1700 cm^{-1} of these metal complexes show no pronounced changes with substitution of the axial ligand. The positions of many of the peaks are difficult to define because of their weakness. The ligand dependence of higher energy peaks must be studied by excitation in the Q bands.

IV. DISCUSSION

A. Electronic Spectra of Porphyrins

The visible and near UV spectra of metal porphyrins can be interpreted using the 4 orbital model proposed by Gouterman and coworkers[27,28]. The electronic transitions that give rise to the characteristic spectra of metal porphyrins [α, β (Q bands) and Soret (B band)] result from excitation from the two highest filled orbitals of a_{2u} and a_{1u} symmetry under the D_{4h} point group to the lowest empty orbitals of e_g symmetry (Fig. 5). The two doubly degenerate excited states that result are of identical symmetry and are nearly degenerate in energy; consequently, they are mixed by configuration interaction to give two new doubly degenerate states resulting from addition or subtraction of the transition dipoles. This leads to a very intense absorption band at high energy, the Soret band, and a less intense band at lower energy, the α band[27,28]. In addition, the 0-1 vibronic overtone (β band) is also active and appears as an additional peak on the high energy side of the 0-0 transition (α band).

The visible and UV spectra of most metalloporphyrins and of the dianion and dication of the free base porphyrins are remarkably similar[29,30,31].

Small changes occur in the position and relative intensities of the α, β and Soret bands, but the spectra are qualitatively similar, indicating little metal-porphyrin interaction. Through an extended Hückel calculation Gouterman and his coworkers[32] have shown that the energies of the porphyrin π orbitals and the metal d orbitals are sufficiently different for most metalloporphyrins that little mixing occurs. For Fe^{3+} and Mn(III) porphyrins, however, the energies of the d orbitals and the porphyrin π orbitals are sufficiently close in energy for large interactions to occur, perturbing the classic metalloporphyrin spectrum[22,32].

Manganese(III) porphyrins exhibit a wealth of absorption bands in the near IR, visible and near UV region. The simple 4 orbital model breaks down for Mn(III) porphyrins. Boucher[20,22] proposed that the additional bands that appear in the absorption spectrum of Mn(III) porphyrins, especially band V, result from charge transfer transitions. These occur when an electron is promoted from a filled porphyrin orbital to an unfilled orbital of the metal or *vice versa*[20,32]. Boucher has assigned the near IR absorption bands of Mn(III) porphyrins to d$\rightarrow$d and/or charge transfer transitions. Prior to this report, the visible bands III and IV were assigned to charge transfer and/or Q transitions. From its sensitivity to solvent and axial ligation, band V was assigned to a charge transfer transition. Low temperature absorption and MCD data[33] indicate that band V spans two electronic transitions, each of which shows an A term in the MCD spectrum. The separation between these transitions, the frequencies at which they occur and their intensities are remarkably dependent on the axial ligand on the manganese[33].

B. Raman Theory

According to Albrecht's theory of Raman intensities[34,35,36] the relevant part of the Raman tensor expression for the intensity of a Raman line corresponding to the vibrational transition $i \to j$ is[36]:

$$(\alpha_{\rho\sigma})_{gi,gj} = \frac{1}{h^2} \sum_{v} \sum_{s} \sum_{a} [\langle g|R_\sigma|e\rangle \langle e|\frac{\partial H}{\partial Q_a}|s\rangle \langle s|R_\rho|g\rangle \langle gi|ev\rangle \langle ev|Q_a|gi\rangle$$

$$+ \langle g|R_\rho|e\rangle \langle e|\frac{\partial H}{\partial Q_a}|s\rangle \langle s|R_\sigma|g\rangle \langle gi|ev\rangle \langle ev|Q_a|gj\rangle]$$

$$\times \frac{1}{(\nu_{ev,gi} - \nu_o + i\Gamma_e)(\nu_s - \nu_e)} \tag{1}$$

for $|s\rangle \neq |e\rangle$,

where $\alpha_{\rho\sigma}$ is the $\rho\sigma$th component of the polarizability tensor and ρ and σ are coordinates within the molecule fixed coordinate system. $|g\rangle$ represents the ground state. $|e\rangle$ represents the excited state in resonance. $|s\rangle$ is a different excited state. $|gi\rangle$ and $|gj\rangle$ are vibrational states of the ground electronic state. $|ev\rangle$ is a vibrational state of the excited electronic state $|e\rangle$. R_ρ and R_σ are the dipole moment operators. $\partial H/\partial Q_a$ is the change in the electronic Hamiltonian with the vibration of the ground state normal mode a. Q_a is the displacement of the ath normal mode. ν_e and ν_s are the energies of the excited states $|e\rangle$ and $|s\rangle$ in frequency units. ν_o is the frequency of the incident laser light. Γ_e is a damping factor.

This equation represents the B term in Albrecht's expression for Raman intensity and results from the vibrationally induced mixing of different electronic states produced by perturbation by the vibrational mode, a. Furthermore, the vibrational mode that is most active in mixing the states will show the greatest Raman intensity. This accounts for the lack of resonance enhancement of vibrations of peripheral substituents in the Raman spectrum of porphyrins. Thus vibrations at the periphery of the ring which do not perturb the electronic states of the porphyrin sufficiently for mixing to occur between different electronic states show little resonance enhancement.

What this argument intends to show is that the enhanced vibrations of a metalloporphyrin with excitation in a charge transfer band are different from the enhanced vibrations with excitation in a $\pi \rightarrow \pi^*$ transition. It is necessary to resolve the spatial properties of $\langle e| \partial H/\partial Q_a |s\rangle$.

The only part of the electronic Hamiltonian that depends on nuclear position is the coulomb potential between electrons and nuclei[34].

i.e. $$(\partial H/\partial Q_a) = -e \sum_j \sum_n \partial(z_n/r_{jn})/\partial Q_a \qquad (2)$$

where the summation is over all of the electrons j and nuclei n, e is the electronic charge, z_n is the charge on nucleus n and r_{jn} is the distance between electron j and nucleus n. $\partial H/\partial Q_a$ is thus a one electron operator. For any one-electron operator, G[34,35,36]:

$$G = -e \sum_j G(r_j) = \int G(r)\rho(r)\, dr \qquad (3)$$

where $G = \partial H/\partial Q_a$

and $$\langle e|G|s\rangle = \langle e|\int G(r)\rho(r)dr|s\rangle = \int \langle e|\rho(r)|s\rangle G(r)dr \qquad (4)$$

where $\langle e|\rho(r)|s\rangle$, the transition density[38], represents the spatial overlap of $|e\rangle$ and $|s\rangle$. As Albrecht has pointed out, for mixing by a vibrational perturbation to occur, the mixed electronic states must lie within the same region of the molecule.

C. Resonance Raman Spectra of Manganese(III) Porphyrins

We will consider excitation within three types of porphyrin transition $\pi \rightarrow \pi^*$, $d \rightarrow d$ and $\pi \rightarrow d$, a charge transfer transition. The results for a $d \rightarrow \pi^*$ charge transfer transition would be the same, but these transitions would not be allowed for Mn porphyrins under D_{4h} symmetry. The ground state for Mn(III) porphyrins is illustrated in Fig. 5:

$$|g\rangle = \Psi_{por}\,\Psi_{metal} = NA\prod_{i}^{m}\phi^{2}_{por_i}\phi^{*o}_{por}d^{1}_{xy}d^{1}_{xz}d^{1}_{yz}d^{1}_{z^2}d^{o}_{x^2-y^2} \tag{5}$$

The lowest energy $\pi\rightarrow\pi^*$ excited states may be written:

$$\left.\begin{aligned} |e\rangle &= N_eA\prod_{i}^{m-1}\phi^{2}_{por_i}\phi^{1}_{por_m}\phi^{*1}_{por}d^{1}_{xy}d^{1}_{xz}d^{1}_{yz}d^{1}_{z^2}d^{o}_{x^2-y^2} \\ |s\rangle &= N_sA\prod_{i}^{m-2}\phi^{2}_{por_i}\phi^{1}_{por_{m-1}}\phi^{2}_{por_m}\phi^{*1}_{por}d^{1}_{xy}d^{1}_{xz}d^{1}_{yz}d^{1}_{z^2}d^{o}_{x^2-y^2} \end{aligned}\right\} \tag{6}$$

An excited state reached by a d→d transition may be written:

$$|d\rangle = N_dA\prod_{i}^{m}\phi^{2}_{por_i}\phi^{*o}_{por}d^{1}_{xy}d^{o}_{xz}d^{1}_{yz}d^{1}_{z^2}d^{1}_{x^2-y^2} \tag{7}$$

The electron is promoted from one of the degenerate d orbitals to the $d_{x^2-y^2}$ orbital. Although there are no d→d transitions allowed under D_{4h} symmetry, a d→d transition from one of the degenerate d orbitals to the $d_{x^2-y^2}$ orbital is allowed under C_{4v} symmetry. The change from D_{4h} to C_{4v} symmetry in a metalloporphyrin can occur by axial ligation. An excited state reached by an allowed charge transfer excitation of an electron from the porphyrin to the metal may be written

$$|c\rangle = N_cA\prod_{i}^{m-1}\phi^{2}_{por_i}\phi^{1}_{por_m}\phi^{*o}_{por}d^{1}_{xy}d^{1}_{xz}d^{2}_{yz}d^{1}_{z^2}d^{o}_{x^2-y^2} \tag{8}$$

Ψ_{por} and Ψ_{metal} represent the wavefunction of the porphyrin and metal, respectively, $|e\rangle$ is the excited state in resonance. N is the normalization factor. A is the antisymmetrizer. ϕ_{por_i} are the occupied molecular orbitals in the ground state configuration of the porphyrin. ϕ^{*}_{por} is the lowest unoccupied porphyrin molecular orbital. The product of orbitals is in order of increasing energy[20]. $d_{xy}, d_{xz}, d_{yz}, d_{z^2}, d_{x^2-y^2}$ represent the atomic orbitals of the manganese. The superscripts indicate the electron occupancy of the orbitals.

An examination of the transition density matrix element indicates which vibrational modes are enhanced by excitation within a particular type of electronic transition. The types of transition density matrix elements that must be examined are between states reached by $\pi\rightarrow\pi^*$ transitions, charge transfer transitions and d→d transitions.

If the two states $|e\rangle$ and $|s\rangle$ that couple are both reached by a $\pi\rightarrow\pi^*$ transition:

$$\langle e|\rho(r)|s\rangle = -e\int \phi^{1}_{por_{m-1}}\delta(r-r_j)\phi^{1}_{por_m}dr_j \qquad (9)$$

since the integral equals unity for electrons not involved in the transition. This is a spatial integral over the two highest energy occupied molecular orbitals of the ground state. Spatially, these orbitals occur within the porphyrin macrocycle and occupy similar regions; as a result, the vibrational modes, a, that are picked out by the electron density matrix element $\langle e|\partial H/\partial Q_a|s\rangle$ are those within the macrocycle.

For coupling of a charge transfer band in which an electron goes to a d_{yz} or d_{xz} orbital, for example, with an excited state reached by a $\pi\rightarrow\pi^*$ transition from the same occupied molecular orbital, the required vibrational perturbation matrix element is $\langle c|\partial H/\partial Q_a|e\rangle$ and the transition density is:

$$\langle c|\rho(r)|e\rangle = -e\int d^{1}_{yz}\delta(r-r_j)\phi^{*1}_{por}dr_j \qquad (10)$$

This integral represents the spatial overlap of a d orbital of the metal and a π orbital of the porphyrin. The region of maximum overlap will occur around the metal and pyrrole nitrogens. The vibrational modes picked out by the transition density operator in this case will be those around the central metal, such as vibrations involving the manganese-pyrrole nitrogen bonds. Vibrations involving the axial ligand on the manganese may also be picked out, because the metal-ligand vibration should perturb the d orbitals, affecting the excited state reached by the charge transfer transition.

For coupling of two different excited states formed by charge transfer transitions in which the excitation is from the same porphyrin ground state occupied molecular orbital, then

$$\langle c_1|\rho(r)|c_2\rangle = -e\int d_1^1\delta(r-r_j)d_2^1 dr_j \tag{11}$$

where $|c_1\rangle$ and $|c_2\rangle$ represent two different charge transfer states and d_1 and d_2 are the two different d orbitals that are occupied by the promoted electron. This term will be small since the two different d orbitals occupy different regions of space, unless axial ligand vibrations and the constraints imposed by the pyrrole nitrogens mix the d orbitals. This may be the term that allows the vibrations of axial ligands to be enhanced. For coupling between two charge transfer states $|c_1\rangle$ and $|c_3\rangle$ that terminate in the same d orbital but are initiated from different porphyrin π orbitals

$$\langle c_1|\rho(r)|c_3\rangle = -e\int \phi^1_{por_m}\delta(r-r_j)\phi^1_{por_{m-1}} dr_j \tag{12}$$

and vibrations active in the macrocycle will show intensity. States differing by the occupancy of more than one electron cannot couple under the vibrational perturbation so that charge transfer transitions differing in occupancy of both porphyrin and d orbitals cannot couple.

Coupling may not occur between a state $|d\rangle$, reached by a $d\rightarrow d$ transition and a state $|e\rangle$, reached by a $\pi\rightarrow\pi^*$ transition because a difference in occupancy of two electrons exists between the two states. State $|d\rangle$ may couple with a charge transfer state $|c\rangle$ if the electron is promoted to the same d orbital in both transitions. The vibrations picked out by this transition density matrix element involve the central metal.

Looking at the form of the polarizability tensor for excitation within (1) a charge transfer band and (2) a $\pi\rightarrow\pi^*$ transition we find:

1. There are terms in the polarizability tensor containing $\langle c|\rho(r)|d\rangle$, $\langle c|\rho(r)|s\rangle$ and $\langle c_1|\rho(r)|c_2\rangle$. The $\langle c|\rho(r)|s\rangle$ and $\langle c|\rho(r)|d\rangle$ terms enhance vibrations active about the metal while the $\langle c_1|\rho(r)|c_2\rangle$ terms enhance vibrations both within the macrocycle and around the metal, including vibrations involving the axial ligand.

2. There are terms containing both $\langle e|\rho(r)|s\rangle$ and $\langle e|\rho(r)|c\rangle$. $\langle e|\rho(r)|s\rangle$ enhances vibrations active in the macrocycle, while $\langle e|\rho(r)|c\rangle$ enhances vibrations about the metal.

In this argument we have neglected configuration interaction of the Q and B states but, as Gouterman[27,28,29] has pointed out, this is a major phenomenon in porphyrins; as a result the B and Q states are mixed and the excited states should be written more precisely:

$$|Q\rangle = M|Q^\circ\rangle + N|B^\circ\rangle \quad \text{and} \quad |B\rangle = P|B^\circ\rangle + T|Q^\circ\rangle$$

where M,N,P and T are the coupling coefficients and $|Q^\circ\rangle$ and $|B^\circ\rangle$ are the zero order $|Q\rangle$ and $|B\rangle$ states. The transition density matrix elements are then:

$$\langle Q|\rho(r)|B\rangle = MT\langle Q^\circ|\rho(r)|Q^\circ\rangle + NP\langle B^\circ|\rho(r)|B^\circ\rangle + (MP+NT)\langle B^\circ|\rho(r)|Q^\circ\rangle \quad (13)$$

The overlap of the $|Q\rangle$ and $|B\rangle$ states with themselves would equal unity. As a result the terms in the polarizability tensor containing $\langle Q|\rho(r)|B\rangle$ would dominate and, for excitation in a Q band we would expect to see vibrations in the porphyrin macrocycle as the major enhanced vibrations.

The contributions from Albrecht's A term[40] in which $|e\rangle = |s\rangle$, the diagonal parts of the transition density matrix element, show similar features. The vibrations that mix an excited porphyrin state with itself must be vibrations within the macrocycle, while the vibrations mixing a charge transfer state with itself must include both vibrations active in the macrocycle and vibrations active around the metal. Since there is no electron interchange between the metal and the porphyrin during a $\pi\to\pi^*$ or $d\to d$ transition, a metalloporphyrin may be treated as two separate systems for these transitions, the metal and the porphyrin ring. For excitation in a $\pi\to\pi^*$ transition, the A term would emphasize vibrations in the macrocycle. With excitation in a $d\to d$ transition, vibrations about the metal would be emphasized, including axial ligand vibrations.

V. CONCLUSION

The above arguments provide a means of distinguishing a charge transfer band from a $\pi\to\pi^*$ transition. The vibrations most enhanced by excitation in band V are vibrations involving the central metal while the vibrations most enhanced by excitation in bands III and IV are porphyrin macrocycle vibrations. Thus, band V is assigned to a charge transfer transition, and bands III and IV are identified as the α and β bands of metalloporphyrins, respectively.

A comparison of the resonance Raman spectra of MnETP in bands III and IV with the resonance Raman spectra of CuETP(I) also favors these assignments (13). The resonance Raman spectra of CuETP(I) excited in the α and β bands show many similarities to the Raman spectra of MnETP excited in bands III and IV. In all of these spectra the enhanced vibrations are those of the porphyrin macrocycle. The vibrations at 757, 988 and 1313 cm^{-1} in MnETP are maximally enhanced with excitation in band III. Analogously, vibrations at 754, 984 and 1314 cm^{-1} in the spectra of CuETP(I) are maximally enhanced with excitation in the α band. The vibration at 1374 cm^{-1} in MnETP shows maximum enhancement with excitation in band IV. The corresponding vibration in CuETP(I) at 1380 cm^{-1} shows maximum enhancement with excitation in the β band.

Many of the low energy vibrations enhanced by excitation in the charge transfer band are metal and axial ligand dependent. Some of these vibrations may be assigned to manganese-halide stretches. The intensity but not the frequency of the vibration at 329 cm^{-1} is strongly dependent on the axial ligand (Fig. 3). Therefore, it may be assumed that this band is only indirectly influenced by the axial ligand. One possible way to account for this intensity dependence is to assume that the 329 cm^{-1} peak is an out-of-plane vibrational mode of the manganese porphyrin. As the ligand increases in size the metal is pulled out of the plane of the porphyrin[15,41]. When the metal lies farther out of the plane, an out-of-plane vibration which puts the metal back into the ring will show increasing enhancement. This could be due to increased coupling between the excited charge transfer state and the π^* state.

The out-of-plane distance of the metal with respect to the porphyrin also has an effect on the extinction coefficient[22,26,41]. For the fluoride complex the ratio of band V to band VI is high. It decreases as the size of the anion increases (Table I). That this must be an effect of the out-of-plane distance of the metal and is not an effect of the ligating atom can be shown by a comparison of the absorption spectra of MnETP with imidazole and piperidine as ligands. Nonbonded interaction of the N-H with the porphyrin ring forces the metal further out of the ring in the piperdine complex than in the imidazole complex[41]. The extinction coefficient of band V in the piperidine complex is only 60% of the value for the imidazole complex. The further the metal lies out of the plane of the porphyrin the more unfavorable is d and π orbital overlap and the less allowed the transition will be.

After completion of this work a report on the resonance Raman spectra of manganese(III) tetraphenyl porphyrin appeared in the literature[17]. This report also noted selective enhancement of low energy Raman modes upon excitation in band V. However, the intensity pattern of these low energy peaks were radically different. The most prominent feature observed by Gaughan and coworkers was a band at 400 cm^{-1}. Both their report and ours show little dependence of the intensity or energy of this band on the axial ligand. The lack of axial ligand vibrations in the Raman spectra of Mn(III) tetraphenyl porphyrin may reflect a difference in the structure of Mn(III) tetraphenyl porphyrin compared to Mn(III) etioporphyrin, because the chloride as well as the bromide complexes of Mn(III) etioporphyrin I and Mn(III) hematoporphyrin IX show similar Raman spectra when excitation occurs in band V[33].

ACKNOWLEDGEMENTS

We are indebted to Drs. J. Scherer and G. Bailey of Western Regional Labs., Albany, California, and Professor H. Strauss for the use of their instruments, to Drs. L. Rosenthal and G. Bailey for their technical assistance, to Dr. M. Calvin for samples of Mn(III)etioporphyrin and to

Dr. L. Vickery for helpful discussions. This work was supported in part by a grant from the National Science Foundation (GB-36361) and in part by the United States Energy Research and Development Administration.

References

1. T. G. Spiro and T. C. Strekas, J. Am. Chem. Soc. 96, 338 (1974).
2. H. Brunner and H. Sussner, Biochim. Biophys. Acta 310, 20 (1973).
3. T. C. Strekas and T. G. Spiro, J. Raman Spectrosc. 1, 387 (1973).
4. T. Yamamoto, G. Palmer, D. Gill, I. T. Salmeen and L. Rimai, J. Biol. Chem. 248, 5211 (1973).
5. T. C. Strekas, A. J. Packer, T. G. Spiro, J. Raman Spectrosc. 1, 197 (1973).
6. H. Brunner, Biochem. Biophys. Res. Commun. 51, 888 (1973).
7. L. A. Nafie, M. Pézolet, W. L. Peticolas, Chem. Phys. Lett. 20, 563 (1973).
8. M. Pézolet, L. A. Nafie and W. L. Peticolas, J. Raman Spectrosc. 1, 455 (1973).
9. T. C. Strekas and T. G. Spiro, Biochim. Biophys. Acta 278, 188 (1972).
10. W. H. Woodruff, T. G. Spiro and T. Yonetani, Proc. Natl. Acad. Sci., U.S. 71, 1065 (1974).
11. A. L. Verma and H. J. Bernstein, J. Raman Spectrosc. 2, 163 (1974).
12. A. L. Verma and H. J. Bernstein, J. Chem. Phys. 61, 2560 (1974).
13. R. Mendelsohn, S. Sunder, A. L. Verma and H. J. Bernstein, J. Chem. Phys. 62, 37 (1975).
14. A. L. Verma, R. Mendelsohn and H. J. Bernstein, J. Chem. Phys. 61, 383 (1974).
15. R. H. Felton, N. T. Yu, D. C. O'Shea and J. A. Shelnutt, J. Am. Chem. Soc. 96, 3675 (1974).
16. L. D. Spaulding, C. C. Chang, N. T. Yu and R. H. Felton, J. Am. Chem. Soc. 97, 2517 (1975).
17. R. R. Gaughan, D. F. Shriver and L. J. Boucher, Proc. Natl. Acad. Sci. USA 72, 433 (1975).

18. R. Plus and M. Lutz, Spectrosc. Lett. 7, 73, 133 (1974).

19. A. L. Verma and H. J. Bernstein, Biochem. Biophys. Res. Commun. 57, 255 (19744).

20. L. J. Boucher, Coord. Chem. Rev. 7, 289 (1972).

21. G. F. Bailey and R. J. Horvat, J. Am. Oil Chemists Soc. 49, 494 (1970).

22. L. J. Boucher, J. Am. Chem. Soc. 92, 2725 (1970).

23. H. Bürger, K. Burczyk and J. H. Fuhrhop, Tetrahedron 27, 3257 (1971).

24. H. Ogashi, Y. Saito and K. Nakamoto, J. Chem. Phys. 57, 4194 (1973).

25. L. J. Boucher and J. J. Katz, J. Am. Chem. Soc. 89, 4703 (1967).

26. L. J. Boucher, J. Am. Chem. Soc. 90, 6640 (1968).

27. M. Gouterman, J. Mol. Spectrosc. 6, 138 (1961).

28. M. Gouterman, Excited States of Matter, Vol. 2, C. W. Shoppee, Ed., pgs. 63-103, Grad Studies, Texas Tech. Univ. (1973).

29. M. Gouterman, J. Chem. Phys. 30, 1139 (1959).

30. C. Weiss, H. Kobayashi and M. Gouterman, J. Mol. Spectrosc. 16, 415 (1965).

31. G. P. Gurinovich, A. N. Sevchenko and K. N. Solovev, in Spectroscopy of Chlorophyll and Related Molecules, AEC-TR-7199, U.S. Atomic Energy Commission, Division of Technical Information.

32. M. Zerner and M. Gouterman, Theoret. Chim. Acta 4, 44 (1966).

33. S. Asher and K. Sauer, unpublished data.

34. A. C. Albrecht, J. Chem. Phys. 34, 1476 (1961).

35. J. Tang and A. C. Albrecht, J. Chem. Phys. 49, 1144 (1964).

36. J. Tang and A. C. Albrecht, in Raman Spectroscopy, Vol. III, Ed. H. A. Szymanski, Plenum Press, N.Y. (1971).

37. J. N. Murrell and J. A. Pople, Proc. Phys. Soc. (London) A69, 245 (1956).

38. H. C. Longuet-Higgins, Proc. Roy. Soc. (London) A235, 537 (1956).

39. H. Ogashi and K. Nakamoto, Bull. Chem. Soc., Japan 44, 49 (1971).

40. A. C. Albrecht and M. C. Hutley, J. Chem. Phys. 55, 4438 (1971).

41. L. J. Boucher, Ann. N.Y. Acad. Sci. 206, 409 (1973).

TABLE I

Absorption maxima (nm) of MnETPX in $CHCl_3$

compared with values reported in the literature

X^- =	F^-		Cl^-		Br^-		I^-	
Band	this study	Ref. (20)	this study	Ref. (20)	this study	Ref. (20)	this study	Ref. (20)
III	582	585	592	592				
IV	550	552	560	559	562	562	568	568
V	450	452	474	474	479	478	492	493
Va			428	427	432	431		
VI	350	356	357	356	361	361	368	368
R	1.30	.72	0.69	.69	.46	.42	.27	.24

$$R = \frac{\text{Abs. peak V}}{\text{Abs. peak VI}}$$

TABLE II

Observed vibrational frequencies and relative intensities of the Raman bands of MnETP in BuOH excited by laser lines at 457.9, 530.9 and 568.2 nm. Relative intensities: vs - very strong; s - strong; m - medium; w - weak; vw - very weak; sh - shoulder.

exciting line: 457.9		530.9		568.2	
$\Delta\nu$, cm^{-1}	I	$\Delta\nu$, cm^{-1}	I	$\Delta\nu$, cm^{-1}	I
				196	vw
		242	w		
266	s	265	vs		
343	vw	342	w	352	vw
398	s	401	w	401	w
				490	vw
600	vw	603	vw	591	vw
683	w	677	w	675	w
		693	w		
		758	w	757	s
803	(solvent)	807	(solvent)	805	(solvent)
		827	(solvent)	828	(solvent)
		849	(solvent)	847	(solvent)
		950	w		
		961	w	960	m
				988	m
		1002	m	1003	m
		1028	w	1028	w

TABLE II (cont.)

exciting line: 457.9		530.9		568.2	
Δν,cm^{-1}	I	Δν,cm^{-1}	I	Δν,cm^{-1}	I
1137	m	1138	m	1136	s
1157	vw	1158	m	1160	s
1220	vw	1220	m	1219	vs
				1271	w
1310	vw	1304	(solvent)	1313	vs
1374	m	1374	s	1376	m
		1407	m	1406	m
		1448	(solvent)	1458	(solvent)
1502	m			1500	w
1566	sh	1566	s	1566	vs
1586	m	1584	vs	1584	vs
1633	w	1633	vs	1633	vs

TABLE III

Observed Raman bands of the halide salts of MnETP. Intensities are labeled as in Table II. All of the vibrational bands listed are polarized.

F^-		Cl^-		Br^-		I^-	
$\Delta\nu, cm^{-1}$	I	$\Delta\nu, cm^{-1}$	I	$\Delta\nu, cm^{-1}$	I	$\Delta\nu, cm^{-1}$	I
						118	s
				143	s		
		165	s				
193		179	s	185	vw	186	w
		225	m			233	s
				245	s	245	w
260		259	m	260	sh	$CHCl_3$	interference
		285	s				
296	w			287	vw		
331	sh	329	s	327	vs	327	vs
343	s	342	s	341	s	340	m
374	vw	373	w	372	w	$CHCl_3$	interference
399	m	398	m	395	m	398	m
495	s						

TABLE IV

Observed vibrational frequencies (cm^{-1}) and shifts of the Raman bands of MnETP ^{35}Cl and ^{37}Cl in CS_2. λ_{ex} = 476.5 nm; $\Delta(\Delta\nu) = \Delta\nu_{^{35}Cl} - \Delta\nu_{^{37}Cl}$

MnETP-^{35}Cl	MnETP-^{37}Cl	$\Delta(\Delta\nu)$
165.7	165.4	
179.9		
226.8	224.2	+2.6
259.0	259.9	
286.5	282.5	+4.0
328.8	329.6	
343.0	343.2	
397.8	398.2	

TABLE V

Assignment of the low energy Raman bands of the MnETP halides

F^-	Cl^-	Br^-	I^-	Assignments
495				
	285			manganese halide stretch
		245		
			233	
374	373	372		porphyrin + manganese
343	342	341	340	porphyrin + manganese
331	329	327	327	out of plane porphyrin + manganese vibration
260	259	260 sh		porphyrin + manganese
	225			porphyrin + Mn + Cl^-
260	162	143	118	porphyrin + Mn + halide

Figure Legends

Fig. 1. Absorption spectrum of Mn(III) etioporphyrin I in butanol. Path length = 1 cm, conc. = 8.34×10^{-4}M. The bands are labeled in Boucher's nomenclature[20,22]. The position and source of the laser lines used in the Raman spectra are indicated.

Fig. 2. a) Resonance Raman spectrum of Mn(III)ETP in butanol. λ_{ex} = 568.2 nm, power = 160 mw. Slit width = 5 cm^{-1}, scan speed = 50 cm^{-1}/min. Conc. ca 10^{-3}M. Because of an increasing background the offset was changed in mid scan. The wavenumber shifts in the figures and tables for all of the Raman spectra in this report were obtained by averaging over several spectra.

b) Resonance Raman spectrum of Mn(III)ETP in butanol. λ_{ex} = 530.9 nm, power = 50 mw. Slit width = 6.4 cm^{-1}, scan speed = 25 cm^{-1}/min. Conc. ca 10^{-3}M.

c) Resonance Raman spectrum of Mn(III)ETP in butanol. λ_{ex} = 457.9 nm, power = 250 mw. Slit width = 6.4 cm^{-1}, scan speed = 50 cm^{-1}/min. Conc. ca 10^{-3}.

Fig. 3. Raman spectra of Mn(III)ETP-X (X-F^-, Cl^-, Br^-, and I^-). CS_2 is the solvent for the F^-, Cl^-, and Br^- complexes. $CHCl_3$ is used for I^- complex. λ_{ex} = 457.9 nm for F^-, 476.5 nm for the Cl^- and 488.0 nm for the Br^- and I^- complexes. Power = 10 mw. Slit width = 5 cm^{-1}, scan speed = 12 cm^{-1}/min. Conc. ca 10^{-3}M. The gaps in the spectrum of MnETP-I indicate solvent interference.

Figure Legends (cont.)

The 260 cm^{-1} shoulder in the spectrum of the bromide complex is more pronounced in other recorded spectra.

Fig. 4. Raman spectra of MnETP-^{35}Cl and ^{37}Cl in CS_2. λ_{ex} = 476.9 nm, power = 10 mw. Slit width = 2 cm^{-1}, scan speed = 1.2 cm^{-1}/min, time constant = 10 sec. Conc. ca 10^{-3}M.

Fig. 5. a) Four orbital model for the electronic transitions of metalloporphyrins.

b) Molecular orbital model for Mn(III) porphyrins[20].

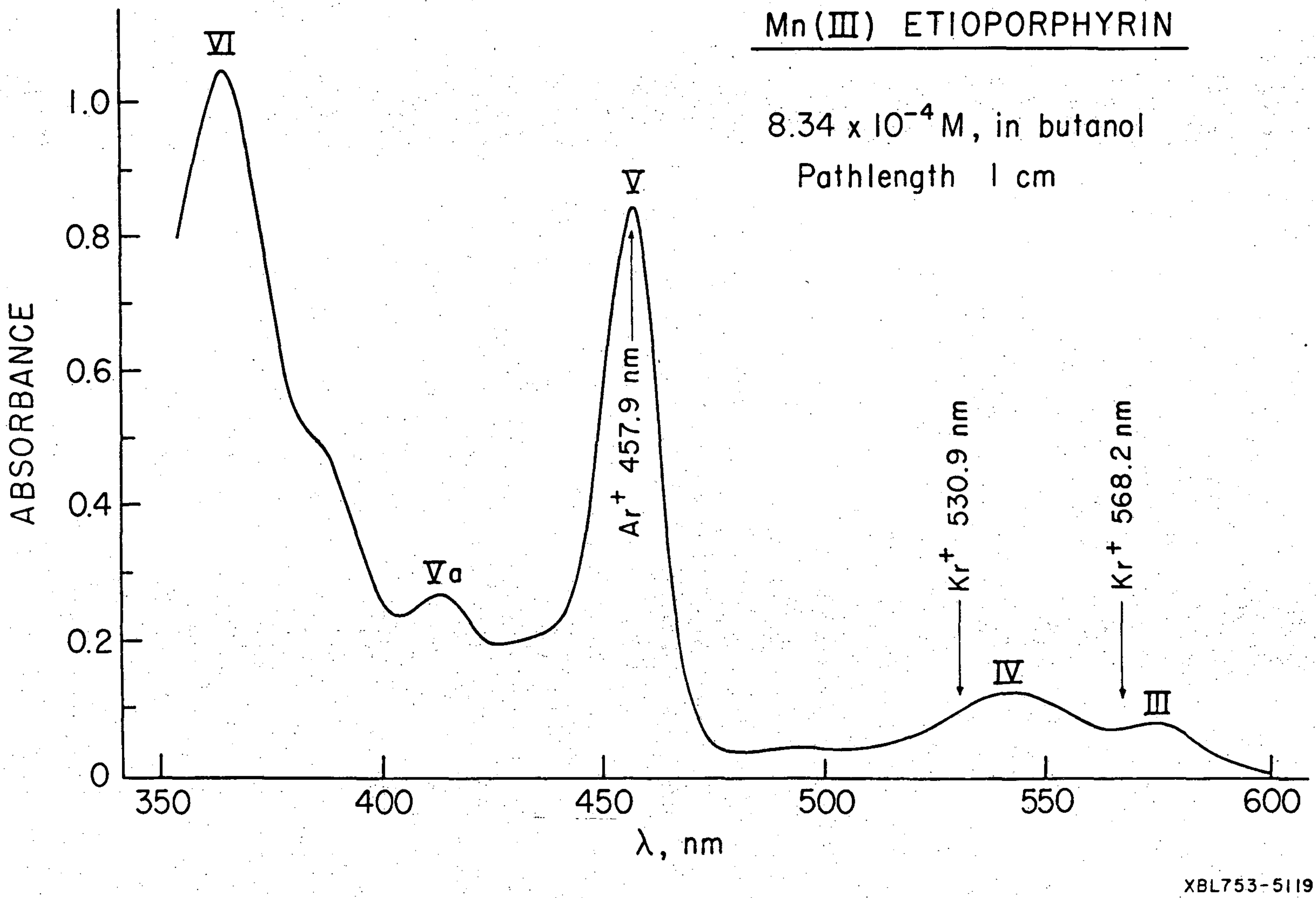

Asher & Sauer

Fig. 1

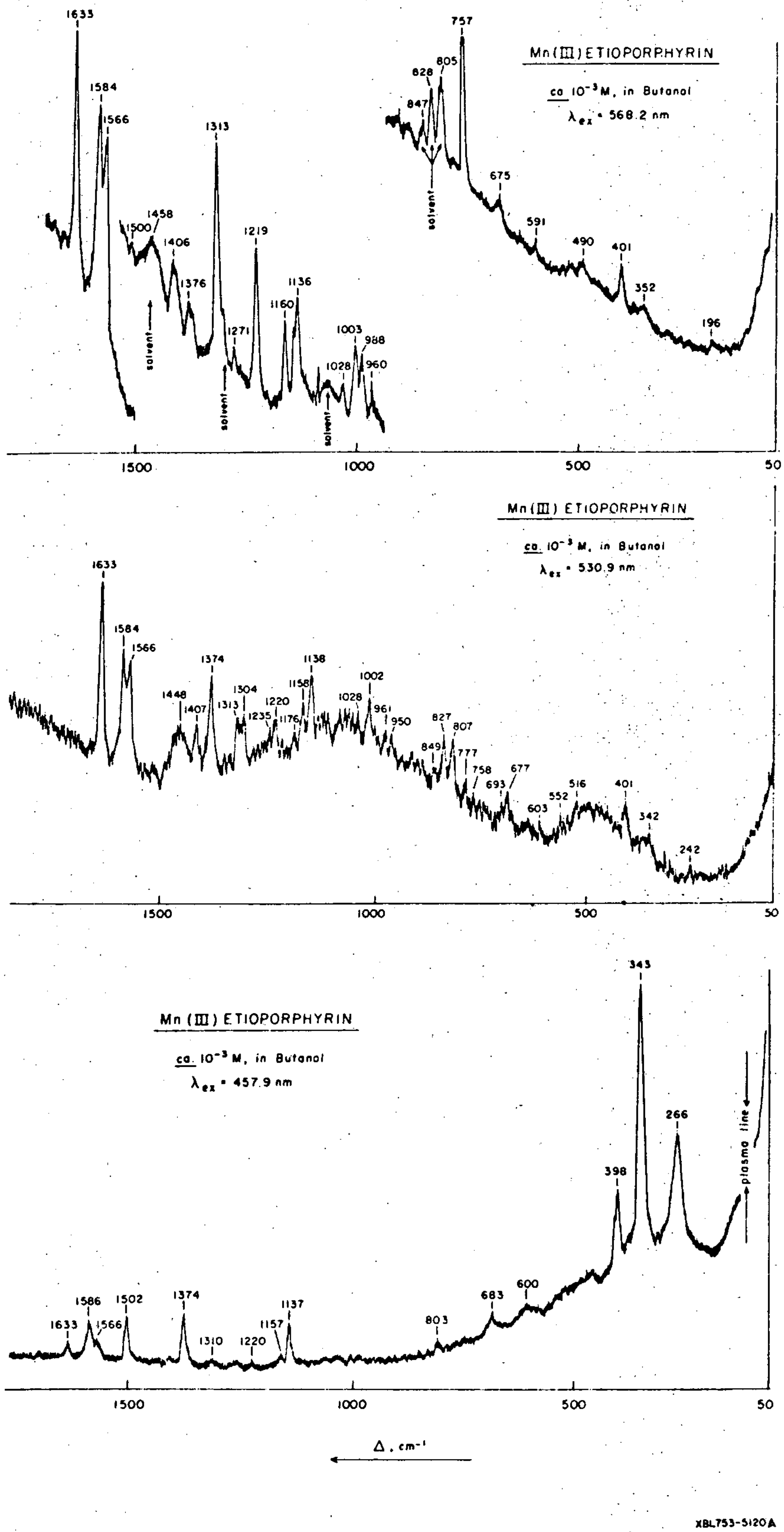

Asher & Sauer

Fig. 2

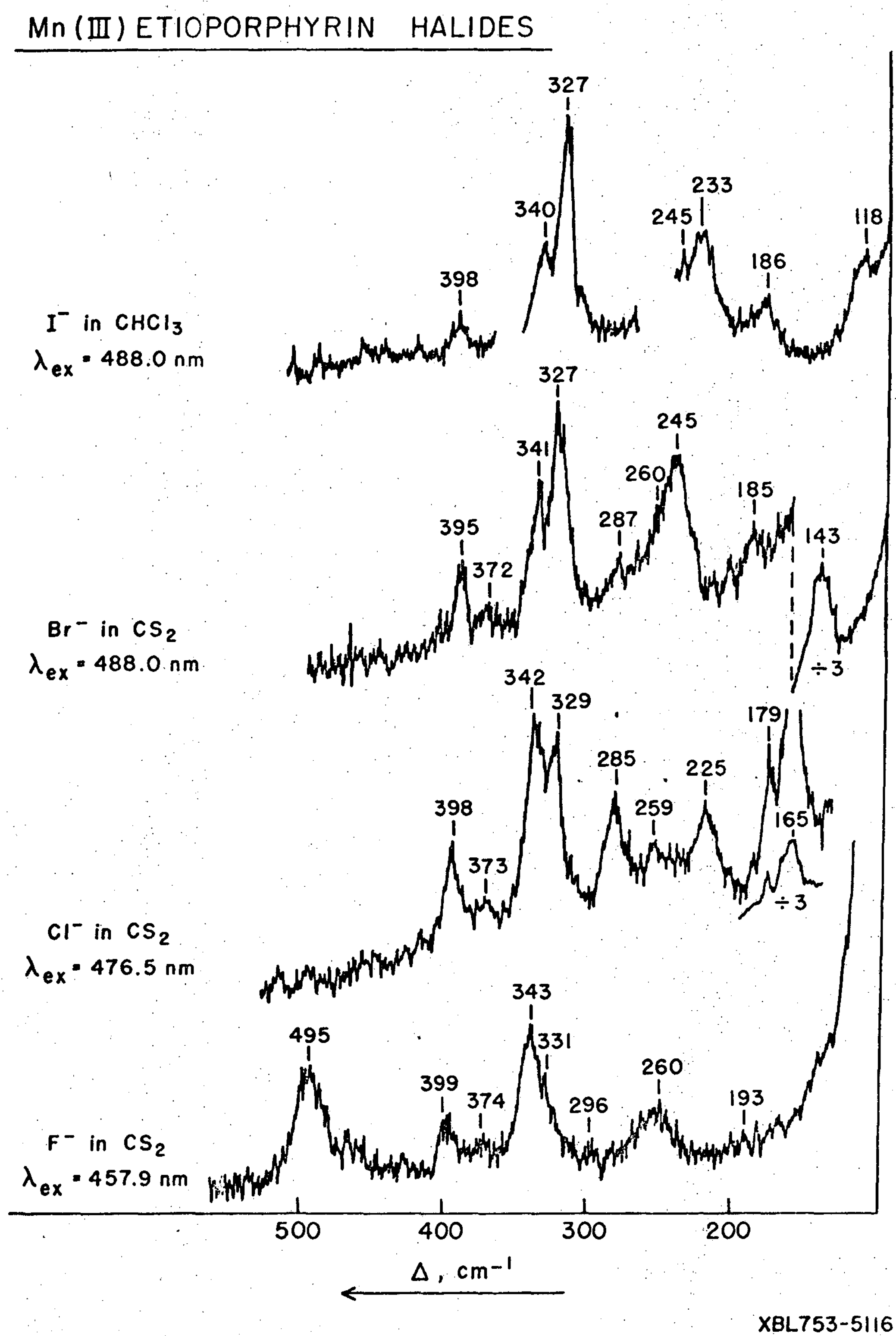

Asher
&
Sauer

Fig. 3

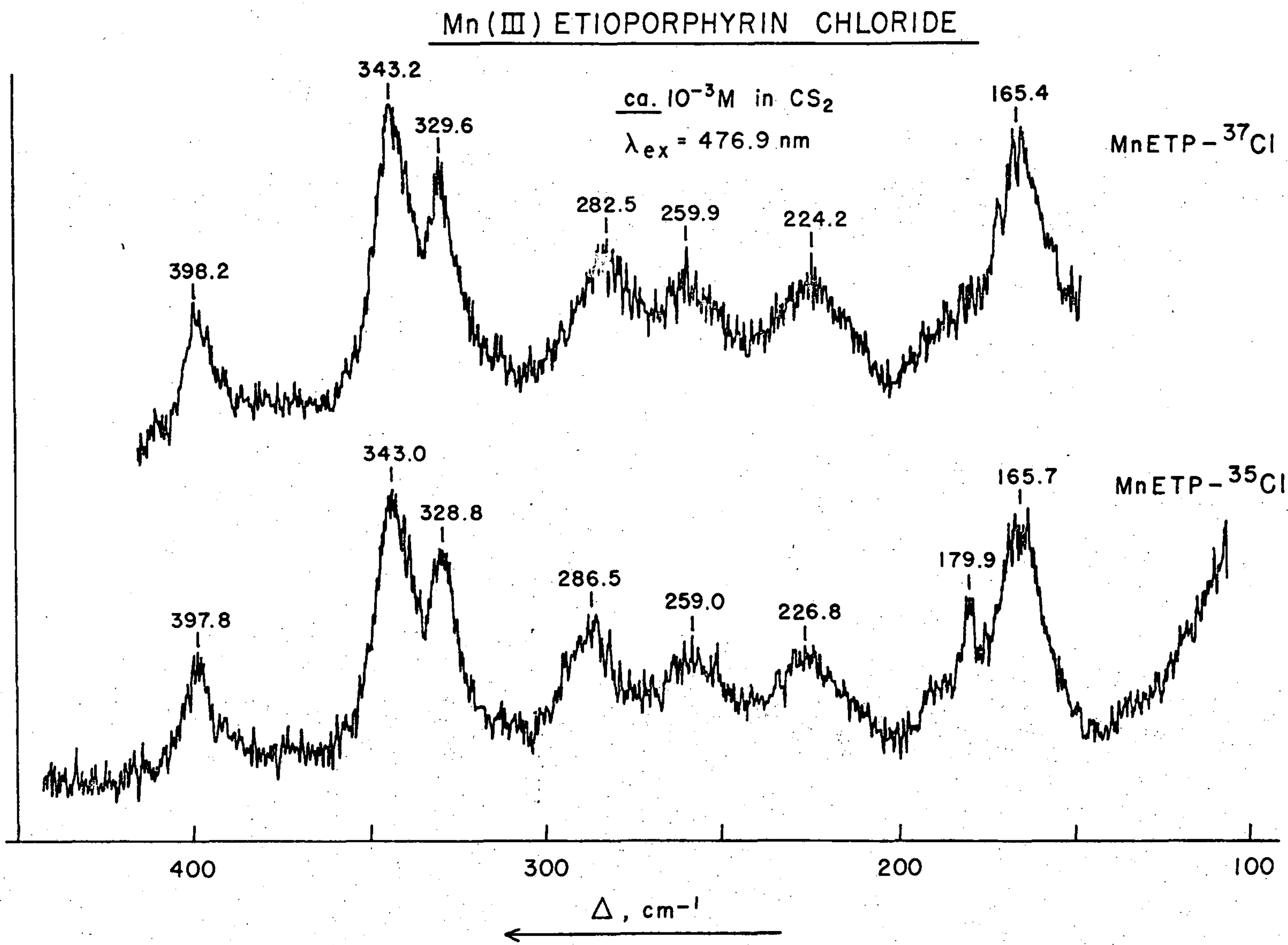

XBL753-5115

Asher & Sauer

Fig. 4

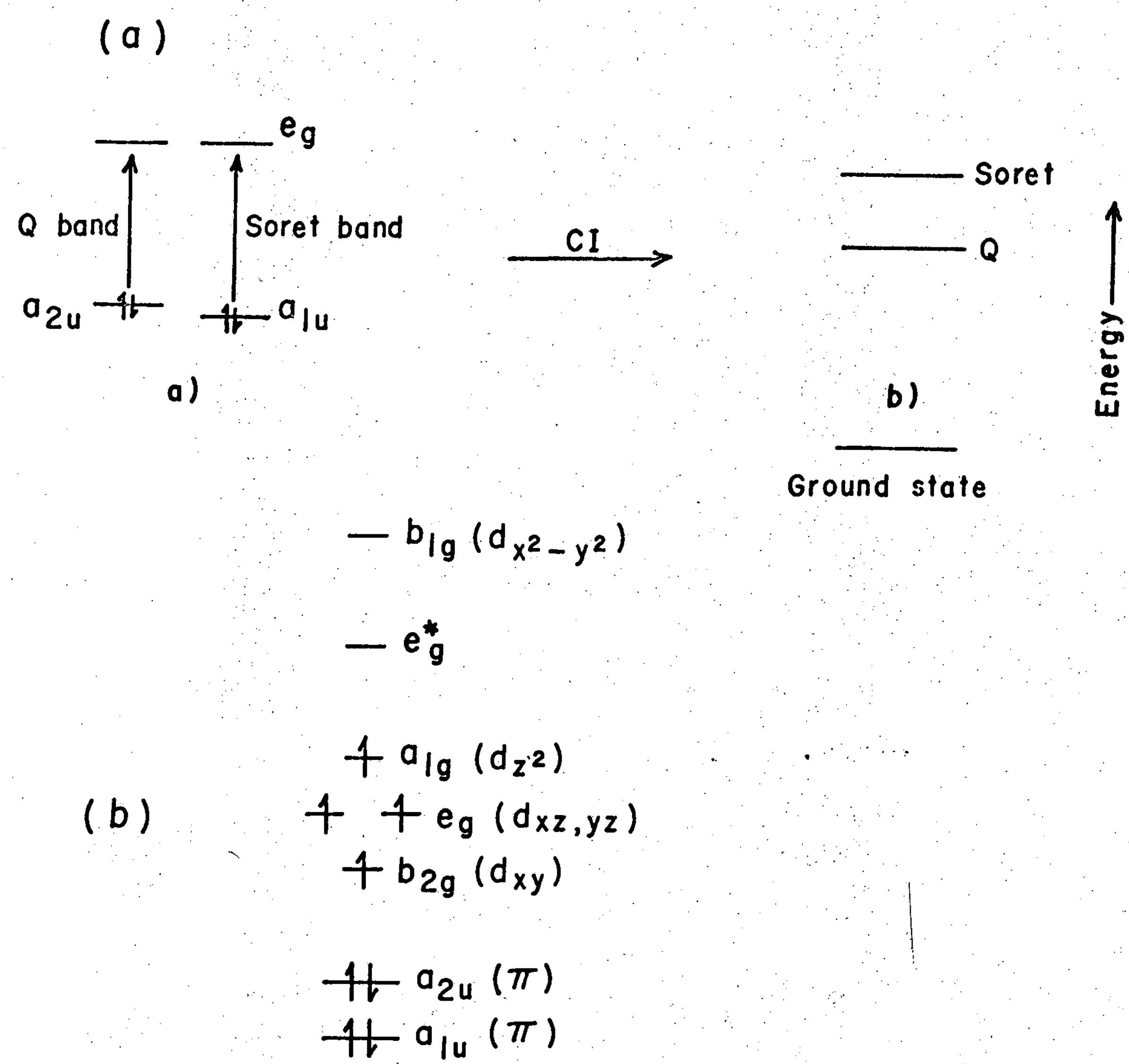

XBL753-5114

Asher
&
Sauer

Fig. 5

TECHNICAL INFORMATION DIVISION
LAWRENCE BERKELEY LABORATORY
UNIVERSITY OF CALIFORNIA
BERKELEY, CALIFORNIA 94720